Decoherence of trapped-atom motional state superpositions[1]

D. J. Wineland,[#] C. Monroe,[‡] C. J. Myatt,[†]
Q. A. Turchette,[§] C. A. Sackett,[*] D. Kielpinski,[¶]
B. E. King,[$] and W. M. Itano[#]

[#]*NIST, Boulder, CO, 80303*

[‡]*Dept. of Physics, Univ. Michigan, Ann Arbor, MI 48109-1120*

[†]*Precision Photonics, Boulder, CO, 80301*

[§]*Research Electro-Optics, Boulder, CO, 80301*

[*]*Dept. of Physics, Univ. Virginia, Charlottesville, VA 22904*

[¶]*Dept. of Physics, MIT, Cambridge, MA, 02139*

[$]*NIST, Gaithersburg, MD, 20899-8424*

david.wineland@boulder.nist.gov

Abstract: Experiments that investigate the decoherence of superpositions of motional states of trapped ions are described. Decoherence is characterized by the loss of contrast in Ramsey-type interferometer experiments involving superpositions of two motional coherent states or two motional Fock states that are subject to stochastically fluctuating electric fields.

1 Introduction

Decoherence in quantum systems [1] has been a subject of enduring interest because its fundamental causes are a subject of debate and more recently because it is *the* problem that must be overcome in quantum information processing [2]. Here, we briefly examine decoherence as it affects quantum superpositions of motional states of a single trapped atom. Since this problem is closely related to decoherence of superposition of states of a single mode of the electromagnetic field, we can rely on a rather large body of theoretical research in quantum optics to guide us; see for example Refs. [3–11].

For brevity, we only summarize the aspects of trapped atomic ion state-manipulation that are relevant for the experiments on $^9Be^+$ ions described below; further details can be found in Ref. [12] and references therein. To a good approximation, a trapped ion can be viewed as being confined in a three-dimensional harmonic well. We consider only motion along one direction; pure states of this motion can be written as superpositions of Fock states

$$\psi_{motion} = \sum_{n=0}^{\infty} C_n|n\rangle, \tag{1}$$

and with laser cooling we will only consider such superpositions for small values of n. The ion has two internal "spin" states that we label $|\downarrow\rangle$ and $|\uparrow\rangle$. The motional and spin states can be manipulated with coherent laser beams through stimulated-Raman transitions. By this means we can perform operations of the form

$$|\downarrow\rangle|n\rangle \rightarrow cos(\theta)|\downarrow\rangle|n\rangle + e^{i\phi}sin(\theta)|\uparrow\rangle|n'\rangle \tag{2}$$

and, in principle, starting from the state $|\downarrow\rangle|n = 0\rangle$, we can synthesize any desired entangled superposition state between the motion and spin [13]. After each experiment, we measure the internal state of the ion, and by repeating the experiment many times we can obtain the probability of finding the ion in the $|\downarrow\rangle$ (or $|\uparrow\rangle$) state.

Decoherence of the ion motion occurs naturally due to ambient fluctuating fields; however, in most cases, for convenience, we can "engineer" the decoherence in order to speed up the experiments.

2 Trapped-ion motional decoherence

We assume that we are interested in characterizing the decoherence of a superposition state $\alpha|\psi_1\rangle + c_2|\psi_2\rangle$ where $|\psi_1\rangle$ and $|\psi_2\rangle$ are states of a single mode of motion (here taken to be the z-mode). This mode of motion we call the quantum "system" under investigation. In a basic model of decoherence [1,3], it is assumed that this state couples to the outside world or "environment," whose initial state is $|\phi_e\rangle$. Therefore, the initial state of the motion and environment can be written $\psi_0 = (c_1|\psi_1\rangle + c_2|\psi_2\rangle) \otimes |\phi_e\rangle$. After the motional state couples to the environment, the system and environment evolve to

$$\psi_0 = (c_1|\psi_1\rangle + c_2|\psi_2\rangle) \otimes |\phi_e\rangle \rightarrow \psi_{final} = c_1|\psi_1'\rangle|\phi_{e1}\rangle + c_2|\psi_2'\rangle|\phi_{e2}\rangle. \tag{3}$$

For a specific type of system/environment coupling, we can assume $|\psi_1'\rangle = e^{i\zeta_1}|\psi_1\rangle$ and $|\psi_2'\rangle = e^{i\zeta_2}|\psi_2\rangle$; therefore, after the interaction, $\psi_{final} = c_1|\psi_1\rangle|\phi_{e1}\rangle + e^{i(\zeta_2-\zeta_1)}c_2|\psi_2\rangle|\phi_{e2}\rangle$ and we see how the initial states become correlated with different states of the environment. Now, if $\langle\phi_{e2}|\phi_{e1}\rangle \simeq 0$, and if the final environment states are uncontrolled and unmeasured (or unmeasurable), we must ignore these degrees of freedom (mathematically trace over them) such that the pure state ψ_{final} becomes a statistical mixture expressed by the density matrix $\rho_{final} = |c_1|^2|\psi_1\rangle\langle\psi_1| + |c_2|^2|\psi_2\rangle\langle\psi_2|$. Hence, the off-diagonal terms or "coherences" of the pure state density matrix $(c_1|\psi_1\rangle + c_2|\psi_2\rangle)(c_1^*\langle\psi_1| + c_2^*\langle\psi_2|)$ are lost to the environment.

It is sometimes useful to incorporate a quantum measuring device or quantum "meter" into the scheme above using a "von Neumann chain" [3]. Here we assume that the quantum system, initially given by $c_1|\psi_1\rangle + c_2|\psi_2\rangle$, is first coupled to a quantum meter and in general, this combination is then coupled to the environment. In the first stage of coupling, we have

$$(c_1|\psi_1\rangle + c_2|\psi_2\rangle) \otimes |\psi_M\rangle \otimes |\phi_e\rangle \rightarrow (c_1|\psi_1'\rangle|\psi_{M1}\rangle + c_2|\psi_2'\rangle|\psi_{M2}\rangle) \otimes |\phi_e\rangle. \tag{4}$$

Upon coupling to the environment, the evolution is

$$(c_1|\psi_1'\rangle|\psi_{M1}\rangle + c_2|\psi_2'\rangle|\psi_{M2}\rangle) \otimes |\phi_e\rangle \rightarrow c_1|\psi_1''\rangle|\psi_{M1}'\rangle|\phi_{e1}\rangle + c_2|\psi_2''\rangle|\psi_{M2}'\rangle|\phi_{e2}\rangle, \tag{5}$$

and, as before, if we assume $\langle\phi_{e2}|\phi_{e1}\rangle \simeq 0$ and that the final environment states are uncontrolled and unmeasured (or unmeasurable), then the final state of the system and meter is expressed by the density matrix

$$|c_1|^2|\psi_1''\rangle\langle\psi_1''||\psi_{M1}'\rangle\langle\psi_{M1}'| + |c_2|^2|\psi_2''\rangle\langle\psi_2''||\psi_{M2}'\rangle\langle\psi_{M2}'|. \tag{6}$$

Therefore the correlation between the system and meter states is established, yielding the expected classical result, and the coherences are lost to the environment. Including the quantum meter more closely describes the ion experiments discussed below because the "system" is the ion's motion, which is not directly measured, but can be coupled to the ion's spin which is the meter that is measured (by laser scattering). In the first experiment described below we will consider a case that is described by expression (5) but we have a situation where $|\phi_{e1}\rangle \simeq |\phi_{e2}\rangle \simeq |\phi_e\rangle$. However since, in practice, we can't measure $|\phi_e\rangle$, and because $|\phi_e\rangle$ changes from experiment to experiment, we must average over the distribution of $|\phi_e\rangle$ states, which leads to decoherence very similar to the case where $\langle\phi_{e2}|\phi_{e1}\rangle \simeq 0$.

2.1 *High-temperature amplitude reservoir*

Decoherence of harmonic oscillator superposition states, with coupling to a variety of reservoir environments, has been investigated extensively in theory; see for example Refs. [3–11]. The model in these studies is a system harmonic oscillator coupled to a bath of environment quantum oscillators. The interaction Hamiltonian for this situation can be modelled as

$$H_I = \hbar \sum_{i=0}^{\infty} \Gamma_i a b_i^\dagger + h.c., \tag{7}$$

where a is the lowering operator for the system oscillator, $b_i^\dagger$ is the raising operator for the ith environment oscillator, and Γ_i gives the strength of coupling between the system oscillator and the ith environment oscillator. The case where the system oscillator is a single mode of the electromagnetic field has been investigated extensively in the experiments of Haroche *et al.* [14]. This model and other similar ones in the specific context of trapped-ion experiments are discussed theoretically in Refs. [12, 15–18]. One model assumes that the motion of a trapped ion couples to the (noisy) uniform electric field $\mathbf{E}$ caused by the environment oscillators through the potential $U = -q\mathbf{x}\cdot\mathbf{E}$, where $\mathbf{x}$ is the displacement of the ion from its equilibrium position. Such a model corresponds to the case of a noisy electric field due to a resistor coupled between the trap electrodes [12, 19], and is described by the Hamiltonian in Eq. (7).

In the experiments, to speed up decoherence, we can simulate a hot resistor coupled between trap electrodes by applying random uniform electric fields that have a spectrum that overlaps the ion's axial-motion frequency ω_z [20, 21]. We generate these fields in the trap by applying voltages to one of the trap electrodes. A commercial function generator produces pseudo-random voltages that are applied through a band-pass filter centered near ω_z, defining the frequency spectrum of the reservoir. We measured the initial coherence and subsequent decoherence of the motion state superpositions with single-atom interferometry, as described in detail in Refs. [20, 21].

Briefly, we first created the entangled system/meter state shown in the left hand side of expression (5) with $|\psi_1'\rangle = |\alpha\rangle, |\psi_{M1}\rangle = |\uparrow\rangle, |\psi_2'\rangle = |\alpha'\rangle, |\psi_{M2}\rangle) = |\downarrow\rangle$, and $c_1 = c_2 = \frac{1}{\sqrt{2}}$ as indicated in part (2) of Fig. 1. Here, $|\alpha\rangle$ and $|\alpha'\rangle$ are coherent states of amplitude α and α'. This state is usually called a "Schrödinger-cat" state. The superposition was then coupled to the reservoir (the applied fluctuating fields) for a fixed time. Finally, the components of the motional-state superposition were overlapped by reversing the steps which initially created it, a final $\pi/2$ pulse was applied to the internal states, and the internal state was measured. The experiment was repeated many times; after each experiment, the internal state of the ion was measured as a function of the relative phase ϕ_R of the creation and reversal steps, and the contrast of the resulting interference fringes characterizes the amount of coherence remaining after coupling to the reservoir. The results are displayed in Fig. 2. We observe that the contrast of the interferometer fringes decays as $\exp(-\kappa|\alpha - \alpha'|^2\langle E_n^2\rangle)$, where $\sqrt{\langle E_n^2\rangle}$ is the r.m.s. value of the applied fluctuating fields and κ is a constant. This scaling was also observed for the ambient fluctuating fields in the experiment [20, 21]. This exponential dependence

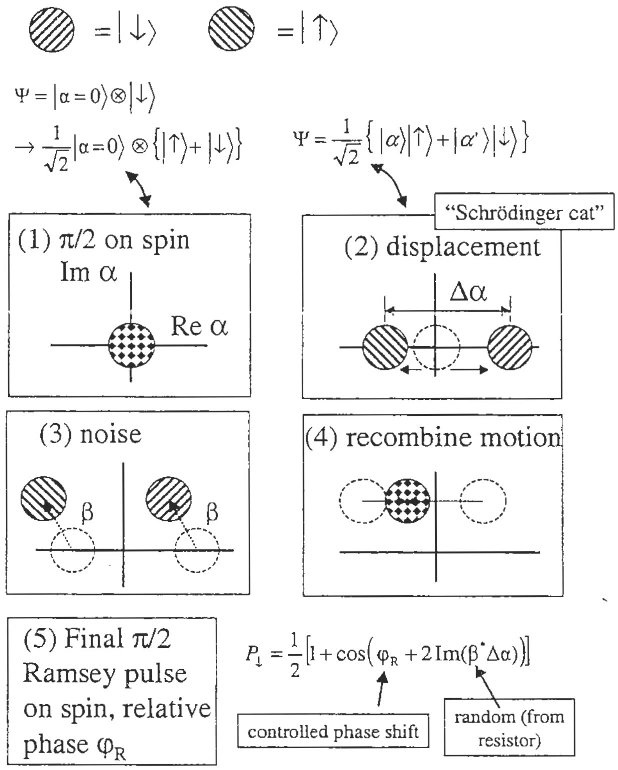

Fig. 1. Pictorial representation in phase space of a Ramsey interferometer [22] experiment designed to observe decoherence of coherent-state superpositions caused by coupling to an amplitude reservoir (from Refs. [20] and [21]). Starting from the initial system/meter state $|\alpha = 0\rangle|\downarrow\rangle$, we create the Schrödinger-cat state shown in panel (2) by applying a $\pi/2$ pulse on the spin followed by a spin-dependent optical-dipole-force displacement [23]. Noise is then applied to the motion simulating coupling to a hot resistor. A (random) displacement β in phase space results as shown in panel (3). Subsequently we reverse the steps used to create the cat state but with a phase shift ϕ_R on the final Ramsey $\pi/2$ pulse. Finally, we measure the probability $P_\downarrow$ of finding the ion in the $|\downarrow\rangle$ internal state. In the absence of noise ($\beta = 0$), we obtain the characteristic sinusoidal oscillations as a function of ϕ_R of Ramsey interferometry; with noise, the Ramsey fringe contrast is reduced because we must average β over a distribution of values characteristic of the applied amplitude noise.

of the decoherence on the "size" of the cat-state $\Delta\alpha \equiv |\alpha - \alpha'|$ agrees with theoretical predictions and indicates why it is so difficult to preserve superpositions except on a microscopic scale.

The decoherence observed here fits into the general scheme outlined above with however some notable differences. First, the environment acted on the system (motional state) and not the meter (spin), so that $|\psi'_{M1}\rangle = |\psi_{M1}\rangle$ and $|\psi'_{M2}\rangle = |\psi_{M2}\rangle$ in expression (5). (Of course, when we finally measured the spin state, we coupled the meter to the environment through laser scattering, but this is not the environment coupling we want to study here.) Also, even though we must have $|\phi_{e1}\rangle \neq |\phi_{e2}\rangle$ because of the difference in back-action from the states $|\alpha\rangle$ and $|\alpha'\rangle$ to the environment, to a very good approximation the back-action of the system on the environment is negligible so that for all practical purposes, $\langle\phi_{e2}|\phi_{e1}\rangle = 1$ and $|\phi_{e1}\rangle = |\phi_{e2}\rangle = |\phi_e\rangle$. Here we have a situation in which we could, in principle, measure $|\phi_e\rangle$ without disturbing it appreciably and apply an operation which undoes its effect. In the case of engineered noise, we could readily do this, but for the case of the ambient noise, this is, in practice, impossible and we must average over the ensemble of environment states $\{|\phi_e\rangle\}$ leading to the expected decoherence exhibited in Fig. 2.

In related experiments discussed elsewhere [20,21], we characterized the decoherence when we applied the same amplitude reservoir to superpositions of two Fock states and also when we apply a phase reservoir, characterized by the interaction Hamiltonian

$$H_I = \hbar a a^\dagger \sum_{i=0}^{\infty} \Gamma_i b_i^\dagger + h.c. \tag{8}$$

to the Schrödinger-cat state and to superpositions of two Fock states.

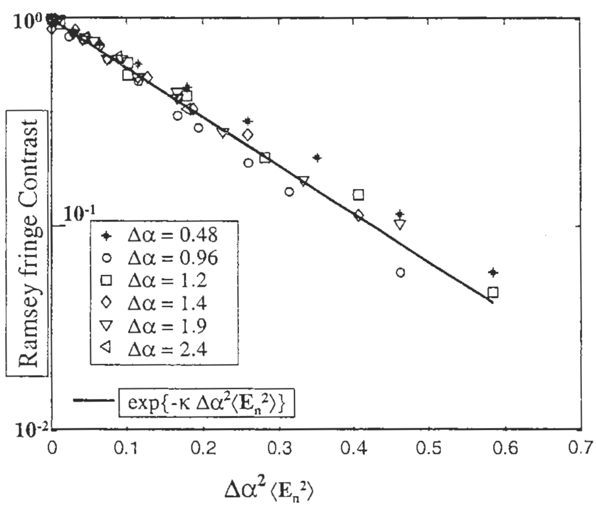

Fig. 2. Loss of coherence of a Schrödinger-cat state caused by coupling to an amplitude reservoir (from Ref. [20]). The amplitude noise was applied for a fixed time interval (3 μs) but with varying amplitude. The contrast for all experiments is normalized to the contrast observed in the absence of applied noise. The expected scaling was observed showing that the decoherence rate is proportional to the square of the phase-space separation $\Delta\alpha$ of the cat-state components.

2.2 *"Engineered" zero-temperature amplitude reservoir*

In the cavity-QED decoherence experiments of Ref. [14], where the system oscillator's frequency is around 50 GHz and the ambient temperature is 0.6 K, the equilibrium oscillator quantum number is around 0.05 and the amplitude reservoir's temperature could be assumed to be 0 K to a good approximation. In the ion experiments, the oscillator's frequency is around 5 MHz and the ambient temperature is near room temperature, implying the equilibrium oscillator number is very large. (Actually, the ambient fluctuating fields behave as if the reservoir were much hotter [24]). Nevertheless, we can simulate a $T = 0$ reservoir, as suggested by Poyatos *et al.* [10]. The basic process is laser cooling as indicated in Fig. 3. Coherent Raman beams couple the states $|\downarrow\rangle|n\rangle \leftrightarrow |\uparrow\rangle|n-1\rangle$ with Rabi rate Ω^*. At the same time, an optical pumping beam causes spontaneous Raman transitions from $|\uparrow\rangle|n\rangle$ to $|\downarrow\rangle|n\rangle$ through the excited P states at rate γ. From the diagram in Fig. 3, we see that all populations are driven towards the state $|\downarrow\rangle|0\rangle$ thereby simulating a $T = 0$ reservoir. By varying the strength of the Raman and optical pumping couplings and time, we have control over the reservoir parameters.

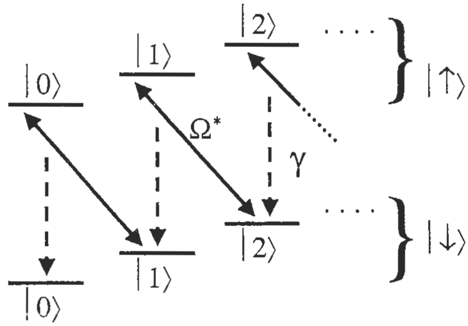

Fig. 3. Schematic diagram depicting an "engineered" T = 0 reservoir. A red sideband drives transitions [20] $|\downarrow\rangle|n\rangle \leftrightarrow |\uparrow\rangle|n-1\rangle$, while spontaneous-Raman scattering is used to make transitions $|\uparrow\rangle|n\rangle$ to $|\downarrow\rangle|n\rangle$ at rate γ. When $\gamma \gg \Omega^*$, the system acts as a $T = 0$ reservoir for motional states.

In the experiments [20, 21], we examined the time evolution of the coherence of the Fock state superposition $\psi = \frac{1}{\sqrt{2}}(|0\rangle + |2\rangle)|\downarrow\rangle$ for varying lengths of reservoir interaction time. To observe this coherence, we made an interferometer similar to one described in the previous section and illustrated in Fig. 4 . (Note that in this experiment, the spin serves multiple functions: it allows us to construct the motional-state interferometer, make measurements and, in the middle of any particular interferometer experiment, it also acts as part of the environment.) The resulting data are shown in Fig. 4. Each data point is the contrast of the interference fringes after the system interacts with the reservoir for a time τ. We show two cases, $\gamma \gg \Omega^*$ and $\gamma < \Omega^*$. In the first case, we observed the decay of the coherence due to coupling to the simulated T=0 reservoir. In this case, it is natural to assume that the reservoir is the spin plus the rest of the environment, which includes the spontaneously scattered photons. (Since we don't rigorously satisfy $\gamma \gg \Omega^*$, we also see some initial non-exponential decay characteristic of the Zeno effect [20, 21]). When $\gamma < \Omega^*$, the coherence between the $|0\rangle$ and $|2\rangle$ state disappears and reappears over time, with an overall decay of the fringe contrast. The underlying effect is population transfer back and forth (Rabi flopping) between the states $|\downarrow\rangle|2\rangle$ and $|\uparrow\rangle|1\rangle$, with a coupling of the $|\uparrow\rangle|1\rangle$ state to the outside environment through spontaneous Raman scattering. If we make $\gamma \to 0$, then we see near perfect revival of the fringe contrast, as expected [21]. For $\gamma \to 0$, we have restricted the environment to be just the internal spin states. In this case, we can reverse the effects of decoherence (of the $\frac{1}{\sqrt{2}}(|0\rangle + |2\rangle)$ state). (A scheme for observing a similar reversal in the context of cavity-QED is discussed in Ref. [25].)

In this experiment, when the atom scatters a photon through spontaneous Raman scattering, no measurement we do will allow us to restore the initial superposition. That is, the emission (and subsequent absorption by a measuring apparatus or the environment) of a spontaneous photon projects the atom into a definite state ($|\downarrow\rangle|1\rangle$ in the context of Fig. 3) and phase information is lost. This is the same situation as in the experiments of Brune *et al.* [14]. The decoherence in this second ion experiment is to be contrasted with the first, where we could in principle detect the environment and reverse its effects. Note that although the data for $\gamma < \Omega^*$ illustrate how coherence transferred to the environment can be recovered, an alternative explanation would say that by transferring the $|\downarrow\rangle|2\rangle$ component of the superposition to the $|\uparrow\rangle|1\rangle$ state, we can gain "which-path" information in our interferometer - the paths being the $|\downarrow\rangle|0\rangle$ and $|\downarrow\rangle|2\rangle$ parts of the superposition. The oscillation in which-path information is analogous to

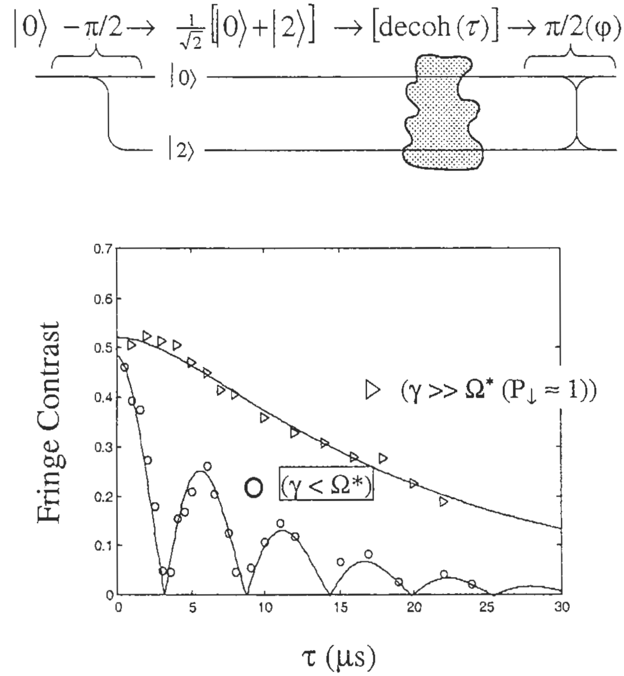

Fig. 4. Decoherence of the motional superposition state $\frac{1}{\sqrt{2}}(|0\rangle + |2\rangle)$ coupled to an engineered $T = 0$ reservoir (from Refs. [20] and [21]). In the upper part of the figure we show schematically how the motional state Ramsey-interferometer works, where the reservoir is applied during the time indicated by the shaded area. In the lower part of the figure, we show the interferometer contrast as a function of time for two cases of the relative values of Ω^* and γ. The initial contrast (without decoherence) is not unity due to imperfections in the motional-state Ramsey interferometer.

that illustrated by the experiments of Chapman *et al.* [26], Dürr *et al.* [27], Kokorowski *et al.* [28], and Bertet *et al.* [29].

This second experiment also illustrates a fundamental dilemma in explaining decoherence. If we restrict the size of the environment to be the spin ($\gamma \to 0$), then the coherence information is not lost and can be recovered, as indicated by the revival of the contrast. Even in the case of photon emission (spontaneous emission at rate γ in Fig. 3), the information need not be lost if the photon is emitted into a lossless cavity where it can be recovered, as illustrated in the cavity-QED experiments [30, 31]. Therefore it seems that decoherence is useful to describe situations, where for practical and technical reasons, we cannot retain the overall system information or the overall system cannot be regarded as being closed. However, these limitations seem only to be practical and not fundamental *unless* some mechanism, that is so far missing in quantum mechanics, can give rise to intrinsic decoherence . For a summary of alternatives, see for example, Ref. [32].

2.3 *Motional decoherence in practice*

The ambient motional decoherence observed in the NIST experiments can be characterized by the model described in the first case above; its characteristics are the same as that caused by thermal electronic noise in the resistance of the electrodes or resistance coupled to the electrodes. At the relatively low ion oscillation frequencies used, where the characteristic wavelength is much larger than the electrode spacing, this could be described by Johnson noise associated with lumped circuit elements attached to the electrodes. Typical heating rates (expressed as quanta per second from the motional ground state) are observed to be around $\langle dn/dt \rangle \simeq 10^3 - 10^4\ s^{-1}$ for $\nu_z \simeq 10$ MHz and the distance from the ion to the nearest electrode surface around 150 μm [24]. The problem is that given our best estimates of the electrode resistance [12] and attached circuit elements, the electrodes would have to be at a temperature of 10^6 K or higher to explain most of the heating results [24]. The principal cause of the anomalously large fluctuating fields and resultant heating is still not understood at this time, but some of its characteristics are known. It appears to be rather broad band (no sharp resonances observed from 2 to 20 MHz) and is likely caused by electric-field noise emanating from the electrodes. For example, heating from collisions due to background gas or an electron field emission source would tend to heat the internal modes of two ions at about the same rate as the center-of-mass (COM) modes. However, we observe that the internal mode heating is negligible compared to the heating of the COM modes [33] indicating that the fields at the site of the ions are approximately uniform spatially. (We note that the experiments of Rohde *et al.* [34] disagree with this finding.). A general trend is that the heating is proportional to $1/R^\kappa$ where $\kappa > 2$. For thermal electronic noise from circuit resistance, $\kappa = 2$ [12]. If the noise were due to fluctuating patch fields, $\kappa = 4$ [24]. The scatter of the data using $^9Be^+$ ions is rather large but is consistent with $\kappa = 4$. Data on other traps [34, 35] appear also to be consistent with κ equal to 4 or more.

In the experiments of Ref. [24], there was some indication that beryllium deposition onto the electrodes caused a higher heating rate. (Beryllium ions are created in the trap by ionizing neutral beryllium atoms that pass near the center of the trap after being emitted from a wide angle source. Some of the beryllium atoms from the source are deposited on electrodes.) By masking the electrodes from direct beryllium deposition, preliminary evidence indicates a significant drop ($\simeq 100$) in heating rate (M. Rowe *et al.*, unpublished). In any case, we conjecture that for clean metal electrode surfaces, free from oxides or adsorbed gases (which could support mobile electrons), the heating should approach that predicted by thermal electronic noise $\langle dn/dt \rangle \simeq 1\ s^{-1}$.

3 Acknowledgements

This work was supported by NSA/ARDA, ONR, and ARO. We thank B. DeMarco, D. Leibfried, M. Lombardi, D. Smith, and D. Sullivan for helpful comments on the manuscript.

References and links

1. W. H. Zurek, "Decoherence, einselection, and the quantum origins of the classical," quant-ph/0105127 (2001).
2. D. P. DiVincenzo, in *Scalable Quantum Computers*, S. L. Braunstein and H. K. Lo, eds., (Wiley-VCH, Berlin, 2001), pp. 1–13.
3. W. H. Zurek, "Decoherence and the transition from quantum to classical," Physics Today **44**, 36–44 (October, 1991).
4. A. O. Caldeira and A. J. Leggett, "Influence of damping on quantum interference: an exactly soluble model," Phys. Rev. A **31**, 1059–1066 (1985).
5. D. F. Walls and G. J. Milburn, "Effect of dissipation on quantum coherence," Phys. Rev. A **31**, 2403–2408 (1985).
6. M. J. Collett, "Exact density-matrix calculations for simple open systems," Phys. Rev. A **38**, 2233–2247 (1988).
7. D. F. Walls and G. J. Milburn, *Quantum Optics*, 1st ed. (Springer, Berlin, 1994).
8. W. Vogel and D. G. Welsch, *Quantum Optics*, 1st ed. (Akademie Verlag, Berlin, 1994).
9. V. Bužek and P. L. Knight, "Quantum interference, superposition states of light, and nonclassical effects," Prog. Opt. **34**, 1–158 (1995).
10. J. F. Poyatos, J. I. Cirac, and P. Zoller, "Quantum reservoir engineering with laser cooled trapped ions," Phys. Rev. Lett. **77**, 4728–4731 (1996).
11. W. P. Schleich, *Quantum Optics in Phase Space*, 1st ed. (Wiley-VCH, Berlin, 2001).

12. D. J. Wineland, C. Monroe, W. M. Itano, D. Leibfried, B. E. King, and D. M. Meekhof, "Experimental issues in coherent quantum-state manipulation of trapped atomic ions," J. Res. Nat. Inst. Stand. Tech. **103**, 259–328 (1998).
13. C. K. Law and J. H. Eberly, "Arbitrary Control of a Quantum Electromagnetic Field," Phys. Rev. Lett. **76**, 1055–1058 (1996).
14. M. Brune, E. Hagley, J. Dreyer, X. Maître, A. Maali, C. Wunderlich, J. M. Raimond, and S. Haroche, "Observing the progressive decoherence of the "meter" in a quantum measurement," Phys. Rev. Lett. **77**, 4887–4890 (1996).
15. S. Schneider and G. J. Milburn, "Decoherence in ion traps due to laser intensity and phase fluctuations," Phys. Rev. A **57**, 3748–3752 (1998).
16. M. Murao and P. L. Knight, "Decoherence in nonclassical motional states of a trapped ion," Phys. Rev. A **58**, 663–669 (1998).
17. S. Schneider and G. J. Milburn, "Decoherence and fidelity in ion traps with fluctuating trap parameters," Phys. Rev. A **59**, 3766–3774 (1999).
18. R. Bonifacio, S. Olivares, P. Tombesi, and D. Vitali, "Model-independent approach to nondissipative decoherence," Phys. Rev. A **61**, 053802–1–8 (2000).
19. D. J. Wineland and H. G. Dehmelt, "Principles of the stored ion calorimeter," J. Appl. Phys. **46**, 919–930 (1975).
20. C. J. Myatt, B. E. King, Q. A. Turchette, C. A. Sackett, D. Kielpinski, W. M. Itano, C. Monroe, and D. J. Wineland, "Decoherence of quantum superpositions through coupling to engineered reservoirs," Nature **403**, 269–273 (2000).
21. Q. A. Turchette, C. J. Myatt, B. E. King, C. A. Sackett, D. Kielpinski, W. M. Itano, C. Monroe, and D. J. Wineland, "Decoherence and decay of motional quantum states of a trapped atom coupled to engineered reservoirs," Phys. Rev. A **62**, 053807–1–22 (2000).
22. N. F. Ramsey, *Molecular Beams* (Oxford University Press, London, 1963).
23. C. Monroe, D. M. Meekhof, B. E. King, and D. J. Wineland, "A "Schrödinger cat" superposition state of an atom," Science **272**, 1131–1136 (1996).
24. Q. A. Turchette *et al.*, "Heating of trapped ions from the quantum ground state," Phys. Rev. A **61**, 063418–1–8 (2000).
25. J. M. Raimond, M. Brune, and S. Haroche, "Reversible decoherence of a mesoscopic superposition of field states," Phys. Rev. Lett. **79**, 1964–1967 (1997).
26. M. S. Chapman, T. D. Hammond, A. Lenef, J. Schmiedmayer, R. A. Rubenstein, E. Smith, and D. E. Pritchard, "Photon scattering from atoms in an interferometer: coherence lost and regained," Phys. Rev. Lett. **75**, 3783–3787 (1995).
27. S. Dürr, T. Nonn, and G. Rempe, "Fringe visibility and which-way information in an atom interferometer," Phys. Rev. Lett. **81**, 5705–5709 (1998).
28. D. A. Kokorowski, A. D. Cronin, T. D. Roberts, and D. E. Pritchard, "From single- to multiple-photon decoherence in an atom interferometer," Phys. Rev. Lett. **86**, 2191–2195 (2001).
29. P. Bertet, S. Osnaghi, A. Rauschenbeutel, G. Nogues, A. Auffeves, M. Brune, J. Raimond, and S. Haroche, "A complementarity experiment with an interferometer at the quantum-classical boundary," Science **411**, 166–170 (2001).
30. X. Maître, E. Hagley, G. Nogues, C. Wunderlich, P. Goy, M. Brune, J. M. Raimond, and S. Haroche, "Quantum memory with a single photon in a cavity," Phys. Rev. Lett. **79**, 769–772 (1997).
31. B. T. H. Varcoe, S. Brattke, M. Weidinger, and H. Walther, "Preparing pure photon number states of the radiation field," Nature **403**, 743–746 (2000).
32. A. J. Leggett, "Quantum theory; weird and wonderful," Physics World **12**, 73–77 (December, 1999).
33. B. E. King, C. S. Wood, C. J. Myatt, Q. A. Turchette, D. Leibfried, W. M. Itano, C. Monroe, and D. J. Wineland, "Cooling the Collective Motion of Trapped Ions to Initialize a Quantum Register," Phys. Rev. Lett. **81**, 1525–1528 (1998).
34. H. Rohde, S. T. Gulde, C. F. Roos, P. A. Barton, D. Leibfried, J. Eschner, F. Schmidt-Kaler, and R. Blatt, "Sympathetic ground-state cooling and coherent manipulation with two-ion crystals," J. Opt. B: Quantum Semiclass. Opt. **3**, S34–S41 (2001).
35. F. Diedrich, J. C. Bergquist, W. M. Itano, , and D. J. Wineland, "Laser Cooling to the Zero Point Energy of Motion," Phys. Rev. Lett. **62**, 403–406 (1989).